Precoding Design for Joint Synchronization and Positioning in 5G Integrated Satellite Communications

Tingting Chen*†, Wenjin Wang*†, Rui Ding‡, Gonzalo Seco-Granados§, Li You*†, and Xiqi Gao*†
*National Mobile Communications Research Laboratory, Southeast University, Nanjing 210096, China
†Purple Mountain Laboratories, Nanjing 211100, China
‡Institute of Telecommunication Satellite, China Academy of Space Technology, Beijing 100094, China
§Telecommunications and Systems Engineering Department, Universitat Autònoma de Barcelona, Barcelona 08193, Spain
Email: {ttchen, wangwj, lyou, xqgao}@seu.edu.cn, greatdn@qq.com, gonzalo.seco@uab.es

GLOBECOM 2021 - 2021 IEEE Global Communications Conference | 978-1-7281-8104-2/21/$31.00 ©2021 IEEE | DOI: 10.1109/GLOBECOM46510.2021.9685480

***Abstract*—The development of an integrated satellite-terrestrial communication network has become one of the focuses in both academic and industry in order to provide genuine seamless coverage. For the integrated satellite and terrestrial 5G communication systems, positioning information of user terminals (UTs) can be beneficial in addressing several challenges. In this paper, we propose to utilize 5G new radio synchronization signals to perform positioning. To simultaneously guarantee synchronization and positioning performances for UTs in any place of a cell coverage, we investigate the precoding design at the satellite side for joint synchronization and positioning (JSP) in 5G integrated satellite-terrestrial networks. By considering the missed detection probabilities and angle of departure estimation for the UTs, we provide the precoding design criteria for synchronization and positioning, respectively. Then we introduce the constraint of equal transmit power on every antenna. Based on the criteria and constraint, we formulate the optimization problem for JSP and exploit the conjugate gradient algorithm under the manifold optimization framework to design the precoder. Simulation results show that the proposed precoder can ensure that JSP achieves satisfactory performances within the whole cell coverage.**

I. Introduction

Recently, with the continuously increasing demands for Internet applications, future communication systems aim to provide global coverage, seamless connectivity, and all-scenario services. In this context, the integrated satellite and terrestrial 5G networks are considered as a promising solution for the future wireless networks, which can take advantage of both the terrestrial and the satellite segments [1]. Meanwhile, in order to deliver broadband interactive data traffic, the multi-beam radiation pattern has been widely implemented in satellite communication (SatCom) systems [2].

For wireless communications in the 5G integrated satellite-terrestrial networks, there are several practical issues that should be taken into consideration, one of which is the positioning problem. It has been identified in 5G new radio (NR) protocols/architectures that positioning information can be beneficial in addressing several challenges in the satellite-5G integrated networks, e.g., Doppler compensation, delay compensation, random access, and uplink power control [3]. Global Navigation Satellite Systems (GNSS) in operation include GPS, GLONASS, Galileo, and BeiDou Navigation Satellite System. However, the user terminal (UT) may not have the capability of GNSS positioning, e.g., in urban scenarios where it is troublesome to have enough GNSS satellites to perform the positioning. Motivated by this, positioning with communication technologies has been investigated over the past decades. In the existing literature, the transmitted signals exploited for positioning are mostly different. For example, the work in [4] addressed the positioning and tracking of moving devices utilizing the time of arrival (ToA) and angle-of-arrival (AoA) obtained from uplink reference signals in 5G ultra-dense networks. The authors of [5] proposed a positioning approach based on the transmitted training sequences in millimeter-wave communication systems. A 3-D positioning algorithm based on the broadcast optical signals was proposed in [6]. Contrary to these literature in the transmitted signals, in this paper, we consider employing 5G NR synchronization signals specified by 3$^{\mathrm{rd}}$ generation partnership project (3GPP) to address the positioning problem. The 5G NR downlink synchronization signal block (SSB) is introduced, comprising the primary synchronization signal (PSS) and secondary synchronization signal (SSS). The PSS and SSS possess good correlation properties allowing accurate time and angle measurements, and thus show great potential for positioning.

In this paper, we investigate the UT positioning based on the NR synchronization signals in the 5G integrated SatCom systems with multi-beam architecture. Furthermore, we propose to design a precoder to optimize the joint synchronization and positioning (JSP) performance of UTs within the whole cell coverage. We investigate the precoding design criteria of synchronization and positioning and introduce the

This work was supported in part by the National Key Research and Development Program of China under Grant 2019YFB1803102, in part by the National Natural Science Foundation of China under Grants 61801114, 61631018, and 61761136016, in part by the Jiangsu Province Basic Research Project under Grant BK20192002, and in part by the Fundamental Research Funds for the Central Universities. The work of G. Seco-Granados was supported in part by Spanish project PID2020-118984GB-I00, and by the Catalan ICREA Academia programme.

constraint of equal transmit power on every antenna. Based on the aforementioned criteria and constraint, we formulate the optimization problem for JSP and exploit the manifold optimization framework to design the precoder.

II. System Model

In order to enable JSP of UTs in the whole cell coverage, a multi-beam SatCom equipped with phased array antennas at the satellite side is considered. The 5G synchronization sequences are transmitted in different satellite beams.

Consider a multi-beam SatCom system with N single-antenna UTs. The transmitter at the satellite side deploys a uniform rectangular array (URA) with M_h antennas in each row and a total number of M_v rows in the vertical dimension ($M = M_h M_v$). There are U UTs to be served simultaneously and $U \leq M$. Let L denote the length of a synchronization sequence. The signal $\mathbf{y}_u \in \mathbb{C}^{1\times L}$ received by the UT u can be given by[1]

$$\mathbf{y} = \mathbf{h}\mathbf{W}\mathbf{X} + \mathbf{z}, \tag{1}$$

where $\mathbf{h} \in \mathbb{C}^{1\times M}$ denotes the downlink channel vector between the UT u and satellite, $\mathbf{W} \in \mathbb{C}^{M\times U}$ denotes the precoding matrix, $\mathbf{X} \in \mathbb{C}^{U\times L}$ is the transmitted synchronization signal in 5G NR, and $\mathbf{z} \in \mathbb{C}^{1\times L}$ is the additive white Gaussian noise (AWGN) vector with i.i.d. $\mathcal{CN}(0, \sigma^2)$ entries.

Consider the typical geometric channel model [7]. In this paper, the channel model is simplified to include only one propagation path. Then the channel vector $\mathbf{h}$ can be given by

$$\mathbf{h} = \alpha\sqrt{M}\mathbf{v}^H(\theta, \phi), \tag{2}$$

where

$$\mathbf{v}(\theta, \phi) = \mathbf{v}^{(v)}(\theta) \otimes \mathbf{v}^{(h)}(\theta, \phi), \tag{3}$$

with the normalized channel steering vector

$$\mathbf{v}^{(v)}(\theta) = \frac{1}{\sqrt{M_v}}\left[1, e^{-j\frac{2\pi}{\lambda}d_v u_v}, ..., e^{-j(M_v-1)\frac{2\pi}{\lambda}d_v u_v}\right]^T, \tag{4}$$

$$\mathbf{v}^{(h)}(\theta, \phi) = \frac{1}{\sqrt{M_h}}\left[1, e^{-j\frac{2\pi}{\lambda}d_h u_h}, ..., e^{-j(M_h-1)\frac{2\pi}{\lambda}d_h u_h}\right]^T. \tag{5}$$

In addition, α is the complex path gain, $u_v = \cos\theta$, $u_h = \sin\theta\sin\phi$, $0 < \theta < \pi$ and $-\frac{\pi}{2} < \phi < \frac{\pi}{2}$ are the angle-of-departure (AoD) towards the UT under consideration in vertical and horizontal dimensions, respectively, d_v and d_h are the distances between two adjacent antenna elements in a row and a column, and λ is the carrier wavelength.

Based on the system model presented above, the synchronization and positioning can be achieved via the observation of $\mathbf{y}$ at the receiver. In the following, we further analyze the precoding design criteria for synchronization and positioning, respectively.

III. Precoding Design Criteria

In this section, the precoding design criteria for synchronization and positioning are provided, respectively, by considering the performances of missed detection (MD) probabilities and AoD estimation within the whole cell coverage.

[1]To simplify the notation, the subscript u is dropped in the following.

A. Criterion for Synchronization

In this paper, we consider the synchronization to be a sequence of binary statistical hypothesis tests [8]. At each timing offset, the hypothesis $\mathcal{H}_1$ means that the received synchronization signal is properly aligned with the transmitted signal. The other hypothesis $\mathcal{H}_0$ represents that the signal is misaligned or absent. Denote the test statistic as $T(\tau)$, where τ is the timing offset. Given the observed signal $\mathbf{y}$, test statistic $T(\tau)$ is evaluated at each timing offset τ. If $T(\tau)$ exceeds the threshold ρ, successful synchronization is claimed. We consider the generalized likelihood ratio test as our synchronization detector [8]. The performance of synchronization is then characterized by the MD probability under the accurate τ. Based on proof in [9], the MD probability can be given by

$$\begin{aligned} P_{\mathrm{MD}} &= \mathbb{P}\{T(\tau) < \rho | \mathcal{H}_1\} \\ &= \mathbb{P}\left\{\frac{\|\mathbf{h}\mathbf{W}\mathbf{X}\mathbf{X}^H + \mathbf{z}_2\|_2^2}{\|\mathbf{z}_1\|_2^2} < \frac{\rho}{1-\rho}\right\}, \end{aligned} \tag{6}$$

where $\mathbf{z}_1 \in \mathbb{C}^{(L-U)\times 1}$ and $\mathbf{z}_2 \in \mathbb{C}^{U\times 1}$ have i.i.d $\mathcal{CN}(0, \sigma^2)$ entries. For purpose of improving the synchronization performances of UTs over all interested AoDs within the entire cell coverage, MD probability fairness over all interested AoDs is taken into account. Following this consideration, the conditions that the precoding matrix should satisfy can be expressed as [9]

$$\mathbf{v}^H(\theta, \phi)\mathbf{W}\mathbf{W}^H\mathbf{v}(\theta, \phi) = U, \quad \forall(\theta, \phi) \in \mathcal{B}. \tag{7}$$

According to (7), we define the desired radiation power pattern $\mathbf{C} \in \mathbb{C}^{P\times Q}$ and the actual discrete generated radiation power pattern $\mathbf{B} \in \mathbb{C}^{P\times Q}$, which can be given by

$$[\mathbf{C}]_{p,q} = U, \tag{8}$$

$$\mathbf{B}^T = \begin{pmatrix} \mathrm{diag}^T(\mathbf{V}_0\mathbf{W}\mathbf{W}^H\mathbf{V}_0^H) \\ \mathrm{diag}^T(\mathbf{V}_1\mathbf{W}\mathbf{W}^H\mathbf{V}_1^H) \\ \cdots \\ \mathrm{diag}^T(\mathbf{V}_{Q-1}\mathbf{W}\mathbf{W}^H\mathbf{V}_{Q-1}^H) \end{pmatrix}, \tag{9}$$

respectively, where

$$\mathbf{V}_q = \begin{pmatrix} \mathbf{v}^H(\theta_0, \phi_q) \\ \mathbf{v}^H(\theta_1, \phi_q) \\ \cdots \\ \mathbf{v}^H(\theta_{P-1}, \phi_q) \end{pmatrix}, \tag{10}$$

the continuous AoDs are discretized to (θ_p, ϕ_q) through sampling, $p = 0, 1, ..., P-1$, $q = 0, 1, ..., Q-1$ and $(\theta_p, \phi_q) \in \mathcal{B}$. Then the correlation matrix is utilized to represent the distance between the actual discrete generated and the desired radiation power pattern. Hence, the precoding design criterion for synchronization can be finally reformulated as

$$\arg\min_{\mathbf{W}} 1 - \frac{\mathrm{tr}\left(\mathbf{B}^T\mathbf{C}\right)}{\|\mathbf{B}\|_F\|\mathbf{C}\|_F}. \tag{11}$$

B. Criterion for Positioning

As illustrated in Fig. 1, with the AoD values (θ, ϕ) of the path and the location of the satellite $\mathbf{s} = [x_s, y_s, z_s]^T$ in the Earth Centered Earth Fixed (ECEF) coordinate system, the unit direction vector from the satellite to the UT can be given by

$$\mathbf{d} = [\sin\theta\cos\phi, \sin\theta\sin\phi, \cos\theta]^T. \tag{12}$$

Then the UT position $\mathbf{p} = [x, y, z]^T$ in ECEF can be given by

$$\mathbf{E}\,(\mathbf{p} - \mathbf{s}) = r\mathbf{d}, \tag{13}$$

In (13), $\mathbf{E}$ is the transformation matrix from ECEF to local tangent coordinate expressed as

$$\mathbf{E} = \begin{pmatrix} -\sin\vartheta & -\cos\mu\cos\vartheta & -\sin\mu\cos\vartheta \\ \cos\vartheta & -\cos\mu\sin\vartheta & -\sin\mu\sin\vartheta \\ 0 & -\sin\mu & \cos\mu \end{pmatrix}^T \tag{14}$$

where ϑ and μ denote the longitude and latitude of the sub-satellite point. In addition, r in (13) denotes the distance between the satellite and UT, which can be calculated by the AoDs (θ, ϕ) and the satellite position $\mathbf{s}$ (The altitude of UT is simplified to be zero).

The crucial aspect of this positioning approach is the unit direction vector $\mathbf{d}$, i.e., the AoDs, which determine the positioning accuracy of UT. For this reason, in the following, we further present the AoD estimation method based on maximum likelihood (ML) and its Cramér-Rao lower bound (CRLB).

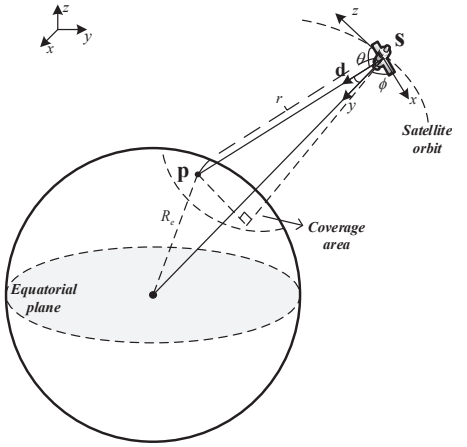

Fig. 1. Illustration of positioning approach in SatCom system.

We model the observation vector $\mathbf{y}$ in (1) as a Gaussian random variable. Given the unknown parameter $\mathbf{r}$

$$\mathbf{r} = [\alpha, \theta, \phi]^T, \tag{15}$$

then the likelihood function of all observations can be expressed as

$$f(\mathbf{y}|\mathbf{r}) = \frac{1}{(\pi\sigma^2)^L} \exp\left\{ -\frac{\|\mathbf{y} - \alpha\mathbf{g}(\theta,\phi)\mathbf{X}\|^2}{\sigma^2} \right\}, \tag{16}$$

where

$$\mathbf{g}(\theta,\phi) = \sqrt{M}\mathbf{v}^H(\theta,\phi)\mathbf{W} \in \mathbb{C}^{1\times U}, \tag{17}$$

which can be derived from (1) and (2).

The ML estimates of the unknown parameter $\mathbf{r}$ are calculated as the maximizing values of $f(\mathbf{y}|\mathbf{r})$. For convenience, the ML estimates are alternatively considered as the minimizing values of the negative log-likelihood function $\log f(\mathbf{y}|\mathbf{r})$. Ignoring the parameter-independent $L\log\pi$-term, we can obtain the equivalent function

$$\begin{aligned} f_l(\mathbf{y}|\mathbf{r}) &= -\log f(\mathbf{y}|\mathbf{r}) = L\log(\sigma^2) \\ &\quad + \frac{1}{\sigma^2}(\mathbf{y} - \alpha\mathbf{g}(\theta,\phi)\mathbf{X})(\mathbf{y} - \alpha\mathbf{g}(\theta,\phi)\mathbf{X})^H. \end{aligned} \tag{18}$$

Hence, the ML parameter estimates can be acquired by solving the minimization problem in the following

$$\hat{\mathbf{r}} = \arg\min_{\mathbf{r}} f_l(\mathbf{y}|\mathbf{r}) \tag{19}$$

Taking derivative of (18) with respect to α and equating it to zero, we can obtain

$$\hat{\alpha} = \frac{\mathbf{y}\mathbf{X}^H\mathbf{g}^H(\theta,\phi)}{\mathbf{g}(\theta,\phi)\mathbf{X}\mathbf{X}^H\mathbf{g}^H(\theta,\phi)}. \tag{20}$$

Substituting (20) into (18), we can then obtain

$$(\hat{\theta}, \hat{\phi}) = \arg\max_{(\theta,\phi)} \frac{(\mathbf{g}(\theta,\phi)\mathbf{X})(\mathbf{y}^H\mathbf{y})(\mathbf{g}(\theta,\phi)\mathbf{X})^H}{(\mathbf{g}(\theta,\phi)\mathbf{X})(\mathbf{g}(\theta,\phi)\mathbf{X})^H}. \tag{21}$$

With (21), the vertical and horizontal AoD estimates can be finally obtained by the high-resolution parameter estimation algorithm in [10]. Then we can back substitute $(\hat{\theta}, \hat{\phi})$ and get our ML estimates $\hat{\alpha}$ from (20).

The CRLB is the minimum variance that an unbiased parameter estimator can attain. In the following, we derive the CRLB to assess the performance of our proposed AoD estimation method. Separating the complex path gain α into real and imaginary parts, we define

$$\mathbf{u} = [\Re\{\alpha\}, \Im\{\alpha\}, \theta, \phi], \tag{22}$$

for which we intend to draw the bounds. The Fisher information matrix (FIM) for complex data can be expressed as [11]

$$[\mathbf{F}(\mathbf{u})]_{ij} = \frac{2}{\sigma^2}\Re\left\{ \mathrm{tr}\left(\frac{\partial\mathbf{R}^H(\mathbf{u})}{\partial u_i} \frac{\partial\mathbf{R}(\mathbf{u})}{\partial u_j} \right) \right\}, \tag{23}$$

where

$$\mathbf{R}(\mathbf{u}) = \alpha\mathbf{g}(\theta,\phi)\mathbf{X}. \tag{24}$$

Then the FIM $\mathbf{F}(\mathbf{u})$ can be given as

$$\mathbf{F}(\mathbf{u}) = \begin{pmatrix} F_{11} & F_{12} & F_{13} & F_{14} \\ F_{12} & F_{22} & F_{23} & F_{24} \\ F_{13} & F_{23} & F_{33} & F_{34} \\ F_{14} & F_{24} & F_{34} & F_{44} \end{pmatrix}, \tag{25}$$

Since the variance of the estimation error can be lower bounded by the diagonal elements of the inverse of FIM for each parameter, CRLB for AoDs can be then calculated as

$$\begin{aligned} \mathrm{CRLB}(\theta) &= [\mathbf{F}^{-1}(\mathbf{u})]_{3,3} \\ &= G(\mathbf{W})/I(\mathbf{W}), \end{aligned} \tag{26}$$

$$\begin{aligned}\mathrm{CRLB}(\phi) &= [\mathbf{F}^{-1}(\mathbf{u})]_{4,4} \\ &= H(\mathbf{W})/I(\mathbf{W}),\end{aligned} \tag{27}$$

respectively, where

$$I(\mathbf{W}) = \det(\mathbf{F}(\mathbf{u})), \tag{28}$$

$$G(\mathbf{W}) = F_{11}^2 F_{44} - F_{14}^2 F_{11} - F_{11} F_{24}^2, \tag{29}$$

$$H(\mathbf{W}) = F_{11}^2 F_{33} - F_{13}^2 F_{11} - F_{11} F_{23}^2. \tag{30}$$

According to (26) and (27), which are functions of the precoding matrix $\mathbf{W}$, the performance of positioning can be characterized by the CRLB. In trying to guarantee the positioning performance of UTs in the entire cell coverage, we focus on the CRLB over all interested spatial directions. Considering AoDs uniformly distributed in $(\theta, \phi) \in \mathcal{B}$, where $\mathcal{B} = [0, \pi] \times [-\frac{\pi}{2}, \frac{\pi}{2}]$ is the coverage region that we are interested in, then the precoding design criterion for positioning can be given by minimizing the integral of CRLB with respect to the whole cell coverage written as

$$\arg\min_{\mathbf{W}} \iint_{\mathcal{B}} \{CRLB(\theta) + CRLB(\phi)\} \, \mathrm{d}\theta \mathrm{d}\phi. \tag{31}$$

IV. Precoding Matrix Design for JSP

Within this part, considering the aforementioned two criteria (11) and (31), we propose to design the precoder based on the dual-objective optimization algorithm.

A. Problem Formulation

Considering the MD probability and AoD estimation accuracy, two precoding design criteria have been summarized in (11) and (31), respectively. According to these criteria, the cost functions $J_1(\mathbf{W})$ and $J_2(\mathbf{W})$ can be defined as

$$J_1(\mathbf{W}) = 1 - \frac{\mathrm{tr}\left(\mathbf{B}^T \mathbf{C}\right)}{\|\mathbf{B}\|_F \|\mathbf{C}\|_F}, \tag{32}$$

$$J_2(\mathbf{W}) = \iint_{\mathcal{B}} \{CRLB(\theta) + CRLB(\phi)\} \, \mathrm{d}\theta \mathrm{d}\phi, \tag{33}$$

respectively.

In order to guarantee the power efficiency at the satellite side, the equal power constraint on precoding matrix $\mathbf{W}$ is introduced, which can be given by

$$\mathbf{I}_M \circ (\mathbf{W}\mathbf{W})^H = \frac{U}{M} \mathbf{I}_M. \tag{34}$$

where the operator $\circ$ denotes the Hadamard product. Hence, the 2-norm of each row of precoding matrix can be the same and the condition of equal average power on every antenna can be satisfied.

Considering the objective functions and the constraint, (32), (33), and (34), the optimization problem to achieve the precoding design can be finally rewritten as a multiobjective optimization problem

$$\begin{aligned} &\text{minimize (with respect to } \mathbf{r}) && (J_1(\mathbf{W}), J_2(\mathbf{W}))^T \\ &\text{subject to} && \mathbf{I}_M \circ \left(\mathbf{W}\mathbf{W}^H\right) = \tfrac{U}{M}\mathbf{I}_M, \end{aligned} \tag{35}$$

where $\mathbf{r} \subseteq \mathbf{R}^2$ is a proper cone ($\mathbf{R}^2$ denotes real 2×1 vectors).

B. Precoding Design for JSP

In order to cope with the multiobjective optimization problem (35), it is convenient to convert the objective vector into a single one. In this paper, we propose a weight sum approach to obtain a combination of the different objectives [12]. Denote the weighted vector as $\boldsymbol{\lambda} = (\lambda_1, \lambda_2)^T$, $\lambda_1, \lambda_2 \geq 0$, and $\lambda_1 + \lambda_2 = 1$. Then (35) can be transformed into a scalar optimization problem written as

$$\begin{aligned} \underset{\mathbf{W}}{\text{minimize}} \quad & J_{ws}(\mathbf{W}|\boldsymbol{\lambda}) = \lambda_1 J_1'(\mathbf{W}) + \lambda_2 J_2'(\mathbf{W}) \\ \text{subject to} \quad & \mathbf{I}_M \circ \left(\mathbf{W}\mathbf{W}^H\right) = \tfrac{U}{M}\mathbf{I}_M. \end{aligned} \tag{36}$$

When $\lambda_1 = 1$, $\lambda_2 = 0$ or $\lambda_1 = 0$, $\lambda_2 = 1$, the JSP optimization problem is degraded into only the MD or AoD optimization. In (36), $J_1'(\mathbf{W})$ and $J_2'(\mathbf{W})$ are the scaling of $J_1(\mathbf{W})$ and $J_2(\mathbf{W})$, respectively, which can be expressed as

$$J_1'(\mathbf{W}) = J_1(\mathbf{W})/\mu_1, \; J_2'(\mathbf{W}) = J_2(\mathbf{W})/\mu_2, \tag{37}$$

where μ_1 and μ_2 are the maximum value of $J_1(\mathbf{W})$ and $J_2(\mathbf{W})$, repectively, so that the range of $J_1'(\mathbf{W})$ and $J_2'(\mathbf{W})$ are both between 0 and 1. In practice, μ_1 and μ_2 can be chosen to be $J_1(\mathbf{W}^0)$ and $J_2(\mathbf{W}^0)$, respectively, where $\mathbf{W}^0$ is the initial precoding matrix of the following iterative method. The optimal solution to (36) is a Pareto optimal point to (35). With different weight vectors in (36), we can obtain a set of different Pareto optimal vectors.

To solve the constrained problem (36), we propose to utilize the conjugate gradient algorithm under the matrix manifold given by

$$\mathcal{N} = \left\{ \mathbf{W} \in \mathbb{C}^{M \times U} : \mathbf{I}_M \circ \left(\mathbf{W}\mathbf{W}^H\right) = \frac{U}{M}\mathbf{I}_M \right\}, \tag{38}$$

which is called the complex oblique manifold.

Under the manifold $\mathcal{N}$, the iterative equation of the precoder matrix can be expressed as

$$\mathbf{W}^{(k+1)} = \mathbf{P}_{\mathcal{N}}(\mathbf{W}^{(k)} + \beta^{(k)} \mathbf{D}^{(k)}), \tag{39}$$

where $\mathbf{W}^{(k)}$ and $\mathbf{W}^{(k+1)}$ represent the precoding matrix acquired at the k-th and $(k+1)$-th iteration, respectively. $\beta^{(k)}$ and $\mathbf{D}^{(k)}$ are the step length and iterative direction for the k-th iteration, respectively. The operator $\mathbf{P}_{\mathcal{N}}(\cdot)$ denotes the projection of a point in the Euclidean space onto the manifold $\mathcal{N}$, which can be formulated as [13]

$$\mathbf{P}_{\mathcal{N}}(\mathbf{W}) = \left(\frac{M}{U} \mathbf{I}_M \circ (\mathbf{W}\mathbf{W})^H \right)^{-1/2} \mathbf{W}. \tag{40}$$

To ensure the sufficient decrease in the objective expression $J_{ws}(\mathbf{W})$ and rule out unacceptably short steps, the line iterative condition stipulates that the step length $\beta^{(k)}$ should satisfy the Wolfe conditions

$$\begin{aligned} J_{ws}(\mathbf{W}^{(k+1)}) \leq & J_{ws}(\mathbf{W}^{(k)}) \\ & + c_1 \beta^{(k)} \Re\left\{ \left\langle \mathbf{D}^{(k)}, \mathrm{grad}_{\mathcal{N}} J_{ws}(\mathbf{W}^{(k)}) \right\rangle \right\}, \end{aligned} \tag{41}$$

Algorithm 1 Precoding Design for JSP

Input: The initial precoding matrix $\mathbf{W}^{(0)}$ and weighted vector $\boldsymbol{\lambda}$

1: Calculte μ_1 and μ_2 by $J_1(\mathbf{W}^{(0)})$ and $J_2(\mathbf{W}^{(0)})$. The initial iterative direction $\mathbf{D}^{(0)} = -\text{grad}_{\mathcal{N}} J_{ws}(\mathbf{W}^{(0)})$.
2: **repeat**
3: **for** all $k > 0$ **do**
4: Calculate the Riemannian gradient $\text{grad}_{\mathcal{N}} J_{ws}^{(k)}$ and iterative direction $\mathbf{D}^{(k)}$ based on (43) and (44), respectively. Calculate the step length $\beta^{(k)}$ until the Wolfe conditions are satisfied.
5: Update $\mathbf{W}^{(k)}$ by (39).
6: **end for**
7: **until** convergence of $\mathbf{W}^{(k)}$

Output: The optimal precoding matrix $\mathbf{W}^* \in \mathcal{N}$

and

$$\begin{aligned}&\Re\left\{\left\langle \mathbf{D}^{(k)}, \text{grad}_{\mathcal{N}} J_{ws}(\mathbf{W}^{(k+1)})\right\rangle\right\} \\ &\quad \geq c_2 \Re\left\{\left\langle \mathbf{D}^{(k)}, \text{grad}_{\mathcal{N}} J_{ws}(\mathbf{W}^{(k)})\right\rangle\right\},\end{aligned} \tag{42}$$

with $0 < c_1 < c_2 < 1$, which are called the Armijo and curvature condition, respectively. In (41) and (42), $\text{grad}_{\mathcal{N}} J_{ws}(\mathbf{W}^{(k)})$ and $\text{grad}_{\mathcal{N}} J_{ws}(\mathbf{W}^{(k+1)})$ represent the Riemannian gradient of $J_{ws}(\mathbf{W}^{(k)})$ and $J_{ws}(\mathbf{W}^{(k+1)})$ on the manifold $\mathcal{N}$, respectively. In the following, we further present the complete expression of the Riemannian gradient on the manifold $\mathcal{N}$ written as [14]

$$\begin{aligned}\text{grad}_{\mathcal{N}} J_{ws}^{(k)} &= \nabla J_{ws}^{(k)} \\ &\quad - \left(\frac{M}{U}\mathbf{I}_M \circ \Re\left\{\mathbf{W}^{(k)}\left(\nabla J_{ws}^{(k)}\right)^H\right\}\right)\mathbf{W}^{(k)},\end{aligned} \tag{43}$$

where ∇J_{ws} is the Euclidean gradient of the objective function $J_{ws}(\mathbf{W})$. The iterative direction $\mathbf{D}^{(k)}$ can be given by the negative Riemannian gradient $-\text{grad}_{\mathcal{N}} J_{ws}^{(k)}$, which is known as the steepest descent method. In this paper, the conjugate gradient method is adopted, which can converge faster than steepest descent method. Then $\mathbf{D}^{(k)}$ is reformulated as

$$\mathbf{D}^{(k)} = -\text{grad}_{\mathcal{N}} J_{ws}^{(k)} + \gamma^{(k)} \mathbf{D}_{+}^{(k-1)}, \tag{44}$$

where $\gamma^{(k)}$ is defined by modified Hestenes-Stiefel rule and $\mathbf{D}_{+}^{(k-1)}$ is $\mathbf{D}^{(k-1)}$ transported to $\mathbf{W}^{(k)}$ given by [14],

$$\begin{aligned}\mathbf{D}_{+}^{(k-1)} =& \mathbf{D}^{(k-1)} \\ &- \left(\frac{M}{U}\mathbf{I}_M \circ \Re\left\{\mathbf{W}^{(k)}\left(\mathbf{D}^{(k-1)}\right)^H\right\}\right)\mathbf{W}^{(k)}.\end{aligned} \tag{45}$$

We detail the precoding design for JSP in Algorithm 1.

V. Numerical Results

In this section, the simulations are provided to evaluate the performance of JSP for 5G integrated SatCom system. The synchronization signal used in simulation is set to be PSS in 5G NR. The other main parameters used in simulations are summarized in Table I.

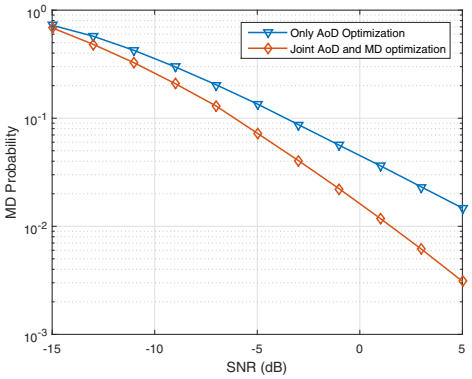

Fig. 2. The MD probabilities with joint optimization and only AoD optimization.

In the simulation part, three representative UT positions (UT 1∼3) are firstly selected within the cell coverage area of the satellite, which are sub-satellite point and two positions at the coverage edge. The satellite position is set to be [7405.3 km, 9.9 km, 727.9 km]^T in low earth orbit (LEO) SatCom systems. The orbital altitude is set to be 1070 km.

TABLE I
Simulation Setup Parameters

Parameter	Value
Subcarrier spacing	15 kHz
System bandwidth	20 MHz
Number of subcarriers	2048
Signal-to-noise ratio	0 dB
Number of antennas at the Tx	8×4
Data stream number of the precoder	3
(λ_1, λ_2)	(0.4,0.6)
Carrier frequency	2.6 GHz

We first study the synchronization performances with our proposed precoding matrices obtained from JSP optimization or only the AoD optimization. The synchronization performances are given by the MD probabilities. To present the MD probabilities over the given signal-to-noise ratio (SNR) ranges, the threshold value ρ in (6) is obtained by the closed-form equation of the false alarm (FA) probability given by [9]

$$P_{FA} = (1-\rho)^{L-1} \sum_{n=0}^{U-1} \frac{(L-1)!}{n!(L-n-1)!} \left(\frac{\rho}{1-\rho}\right)^n. \tag{46}$$

By setting P_{FA} to be 10^{-4}, we can acquire the corresponding threshold value $\rho \approx 0.20127$. Fig. 2 illustrates the MD probabilities with SNR ranging from -15 dB to 5 dB. The simulation result shows that our proposed JSP optimization method has a better synchronization performance than that of only the AoD optimization.

Then we study the positioning performances by analysing the AoD estimation error with our proposed precoding matrices obtained from JSP optimization or only the MD opti-

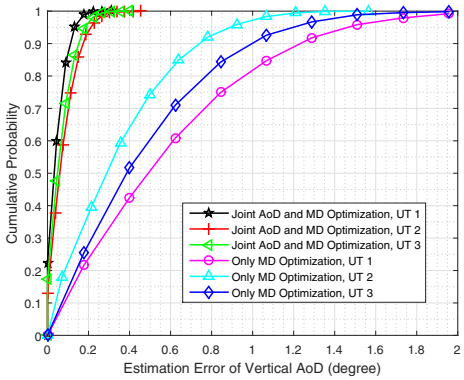

Fig. 3. The cumulative probability distribution of vertical AoD estimation error.

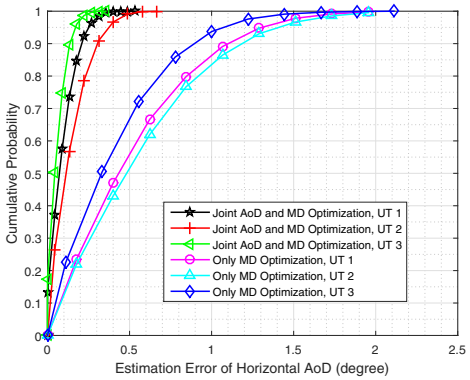

Fig. 4. The cumulative probability distribution of horizontal AoD estimation error.

mization. Fig. 3 and Fig. 4 show the cumulative probability distribution of vertical and horizontal AoD estimation error of different UTs, respectively. From the figures, we can observe that the performances of JSP optimization method in AoD estimation significantly outperforms the performances which only take into account the MD optimization. In addition, Fig. 5 presents the cumulative probability distribution of positioning estimation error with the precoding matrix generated from JSP optimization algorithm. It can be observed that 90% of the position estimates are within the error range of 5 km.

VI. Conclusion

In this paper, we have proposed a precoding design for 5G integrated SatCom system synchronization and positioning. The MD probabilities and CRLB of the AoD estimation algorithm have been employed to formulate the precoding design criteria for synchronization and positioning issues, respectively. The constraint of equal transmit power on every antenna was also considered. With the above criteria and constraint, we introduced the optimization problem for JSP. Then we utilized the conjugate gradient algorithm under the manifold framework to obtain the optimal precoder. Numerical results illustrated that with the proposed precoding matrix,

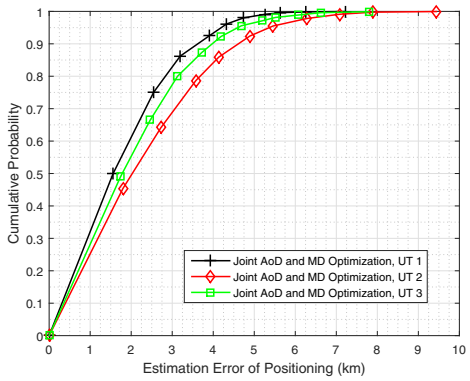

Fig. 5. The cumulative probability distribution of positioning estimation error.

both the synchronization and localization could achieve satisfactory performances under the whole cell coverage.

References

[1] A. Kapovits, M. Corici, I. Gheorghe-Pop, A. Gavras, F. Burkhardt, T. Schlichter, and S. Covaci, "Satellite communications integration with terrestrial networks," *China Commun.*, vol. 15, no. 8, pp. 22–38, Aug. 2018.

[2] L. You, A. Liu, W. Wang, and X. Gao, "Outage constrained robust multigroup multicast beamforming for multi-beam satellite communication systems," *IEEE Wireless Commun. Lett.*, vol. 8, no. 2, pp. 352–355, Apr. 2019.

[3] 3GPP TR 38.811 V15.4.0, "3rd Generation Partnership Project; Technical Specification Group Radio Access Network; Study on New Radio (NR) to Support Non Terrestrial Networks (Release 15)," Tech. Rep., Sep. 2020.

[4] M. Koivisto, M. Costa, J. Werner, K. Heiska, J. Talvitie, K. Leppänen, V. Koivunen, and M. Valkama, "Joint device positioning and clock synchronization in 5G ultra-dense networks," *IEEE Trans. Wireless Commun.*, vol. 16, no. 5, pp. 2866–2881, May 2017.

[5] W. Chen, S. He, Q. Xu, J. Ren, Y. Huang, and L. Yang, "Positioning algorithm and AoD estimation for mmWave FD-MISO system," in *Proc. 2018 WCSP*, Hangzhou, China, 2018, pp. 1–6.

[6] H. Steendam, "A 3-D positioning algorithm for AoA-based VLP with an aperture-based receiver," *IEEE J. Sel. Areas Commun.*, vol. 36, no. 1, pp. 23–33, Jan. 2018.

[7] D. Tse and P. Viswanath, *Fundamentals of Wireless Communication*. Cambridge, U.K.: Cambridge Univ. Press, 2005.

[8] D. W. Bliss and P. A. Parker, "Temporal synchronization of MIMO wireless communication in the presence of interference," *IEEE Trans. Signal Process.*, vol. 58, no. 3, pp. 1794–1806, Mar. 2010.

[9] X. Meng, X. Gao, and X.-G. Xia, "Omnidirectional precoding and combining based synchronization for millimeter wave massive MIMO systems," *IEEE Trans. Commun.*, vol. 66, no. 3, pp. 1013–1026, Mar. 2018.

[10] Fazal-E-Asim, F. Antreich, C. C. Cavalcante, A. L. F. de Almeida, and J. A. Nossek, "Two-dimensional channel parameter estimation for millimeter-wave systems using Butler matrices," *IEEE Trans. Wireless Commun.*, vol. 20, no. 4, pp. 2670–2684, Apr. 2021.

[11] S. M. Kay, *Fundamentals of Statistical Signal Processing: Estimation Theory*. Upper Saddle River, NJ, USA: Prentice Hall, 1993.

[12] Q. Zhang and H. Li, "MOEA/D: A multiobjective evolutionary algorithm based on decomposition," *IEEE Trans. Evol. Comput.*, vol. 11, no. 6, pp. 721–731, Dec. 2007.

[13] P. A. Absil and J. Malick, "Projection-like retractions on matrix manifolds," *SIAM J. Optim.*, vol. 22, no. 1, pp. 135–158, Jan. 2012.

[14] W. Guo, A.-A. Lu, X. Meng, X. Gao, and X.-G. Xia, "Broad coverage precoder design for 3D massive MIMO system synchronization," *IEEE Trans. Commun.*, vol. 68, no. 7, pp. 4233–4246, Jul. 2020.